

A Role of Oxygen Plasma in Growth Enhancements of a-YBCO and Ca-doped Bi2201 Thin Films

N.Hirate, KI.Itoh, S.Yamada, KT.Itoh, M.Tada, K.Ogai, H.Uchikawa, T.Endo, and Y.Tsutsumi*

Faculty of Engineering, Mie University, Tsu, Mie 514-8507, Japan

Fax: 81-59-231-9471, e-mail: endo@cm.elec.mie-u.ac.jp

*Department of Electrical Engineering, Akashi College of Technology, Akashi, Hyogo 674-8501, Japan

Fax: 81-78-946-6138, e-mail: tsutsumi@akashi.ac.jp

Thin films of a-oriented $\text{YBa}_2\text{Cu}_3\text{O}_x$, Ca-doped Bi2201 ($\text{Bi}_2(\text{Sr,Ca})_2\text{CuO}_x$) and nondoped Bi2201 were prepared at 500°C by IBS. The crystal growth of a- $\text{YBa}_2\text{Cu}_3\text{O}_x$ and Ca-doped Bi2201 was enhanced by oxygen plasma supply. This can be interpreted in terms of reduction of surface energy by the plasma. However, the crystal growth of nondoped Bi2201 was improved by oxygen molecular supply. Moderate excitation due to collisions between the supplied oxygen molecules and sputtered particles is effective for this improvement.

Key words: oxide thin films, oxygen plasma, Ca-doped Bi2201, nondoped Bi2201, a-YBCO, surface energy

1. Introduction

We need strong oxidants to prepare perovskite oxide films at low temperatures.^{1),2)} The effective oxygen species are generated in plasma and plume in sputtering and laser ablation techniques. We must, however, supply the activated oxygen in evaporation and MBE techniques. It has been reported by us³⁾ and Sakai et al.⁴⁾ that the activated oxygen is useful in ion beam sputtering (IBS) technique as well. Mukaida and Miyazawa⁵⁾ reported that a growth of a-oriented $\text{YBa}_2\text{Cu}_3\text{O}_x$ (YBCO) is enhanced by the activated oxygen in PLD technique. We reported that a growth of Ca-doped Bi2201 ($\text{Bi}_2(\text{Sr,Ca})_2\text{CuO}_x$) is enhanced by supplying oxygen plasma.⁶⁾

In this paper, we report that oxygen molecules are more effective for preparations of nondoped Bi2201 ($\text{Bi}_2\text{Sr}_2\text{CuO}_x$) but the oxygen plasma is more effective for the Ca-doped Bi2201 and a-YBCO.⁷⁾ According to these results, we suggest that this effect is related to surface energy based on atomic arrangement.

2. Experimental

In order to elucidate the effects of oxidants on the growth of perovskite oxide films, IBS technique was employed.⁶⁾ A target was sputtered by Ar^+ ions at 4 keV, and the sputtered particles were deposited on MgO (100) substrate. Growth rate was in an order of 10^{-2} Å/s. The substrate was heated and the substrate temperature T_s was monitored using a thermocouple. The films were deposited at $T_s=500^\circ\text{C}$ in this work. Averaged oxygen partial pressures P_o were fixed at various values. The oxygen plasma was produced in a plasma source by applying ~ 0.9 kV voltage at 60 Hz and

discharged current of 9.6 mA, and was supplied to the substrate during the film depositions. To clarify the plasma effects, the films were also deposited with supply of oxygen molecules through the same plasma source without the discharge.

We prepared three kinds of films using three different targets. Their compositions are; a) Y/Ba/Cu=1/1.5/2.3, b) Bi/Sr/Ca/Cu=1.6/0.83/0.42/1, and c) Bi/Sr/Cu=2.0/1.2/1. The sample numbers and the deposition conditions are shown in Table I.

Crystallinity of the films was estimated by X-ray diffraction (XRD) on θ - 2θ scan using Cu K α line. The degree of crystallinity was evaluated by FWHM on θ - 2θ peaks of XRD. Surface morphology was estimated by SEM image and AFM analysis. Film thickness was measured by a probe method.

3. Results and Discussion

The XRD patterns of prepared YBCO films are

Table I. Main sample numbers, preparation conditions, film thickness and RMS roughness.

Sample No.	P_o (mTorr)	Deposition time (h)	Thickness (Å)	RMS (Å)
YM	2	6	600	58
YP	2	6	1100	60
BCM	0.75	3	900	341
BCP	0.75	3	1000	346
BM	0.2	6	720	42
BP	0.2	6	840	22

Y:YBCO, BC:Ca-doped Bi2201, B:nondoped Bi2201, M:molecule, P:plasma

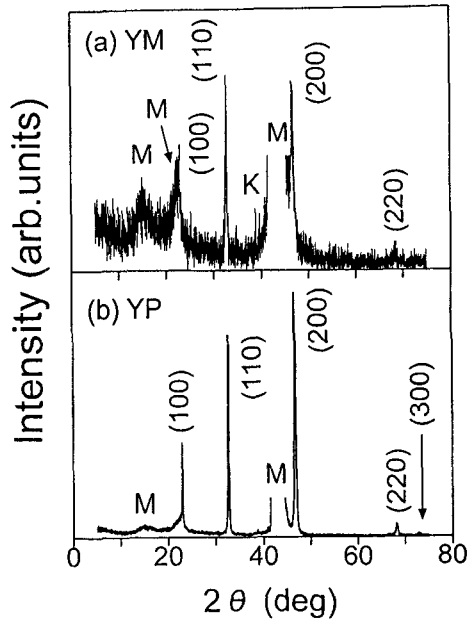


Fig.1. The XRD patterns of YBCO, showing $\text{YBa}_2\text{Cu}_3\text{O}_x$ structure. A plane index is shown for each peak. M, K: MgO peaks.

shown in Fig.1. The films of YM shown in (a) was prepared with the oxygen molecules, and YP in (b) with the oxygen plasma. The both films are mixed with the *a*-phase and (110)-phase. A relative volume fraction γ for each phase is defined using the XRD peaks as

$$\gamma = \frac{\sum \text{peak intensities for each YBCO phase}}{\sum \text{peak intensities for the all YBCO phases}} \times 100.$$

The γ value of the *a*-phase is 44.5% in YM, and it is 60% in YP. Thus the growth of *a*-phase is enhanced by the plasma. The FWHM value of (200) peak is 0.48° in YM, while it is 0.16° in YP. This clearly indicates that the crystallinity is improved by the plasma. The RMS surface roughness is slightly larger for YP than for YM (Table I). However, if the film thickness is taken into account (it is two times thicker for YP than for YM), it can be judged that the surface is smoothed by the plasma.

The XRD patterns of Ca-doped Bi2201 films are shown in Fig.2. The films of BCM shown in (a) was prepared with the molecules, and BCP in (b) with the plasma. The both films are *c*-oriented Bi2201 phases but BCP shows much more excellent XRD pattern than BCM. The FWHM values of

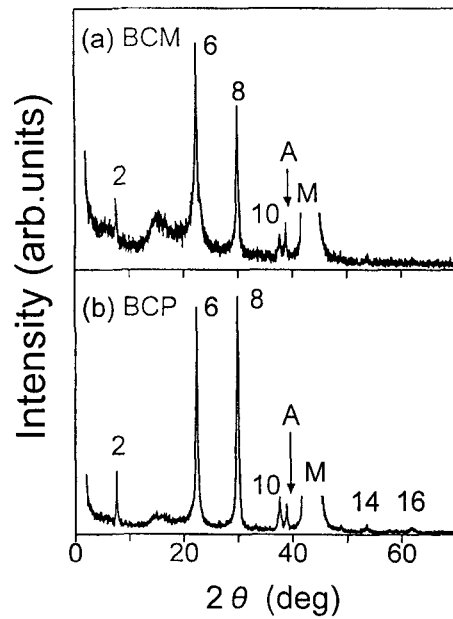


Fig.2. The XRD patterns of Ca-doped Bi2201, showing *c*-oriented Bi2201 phase. A number attached to each peak represents ℓ of (00ℓ) . A: CuO peak.

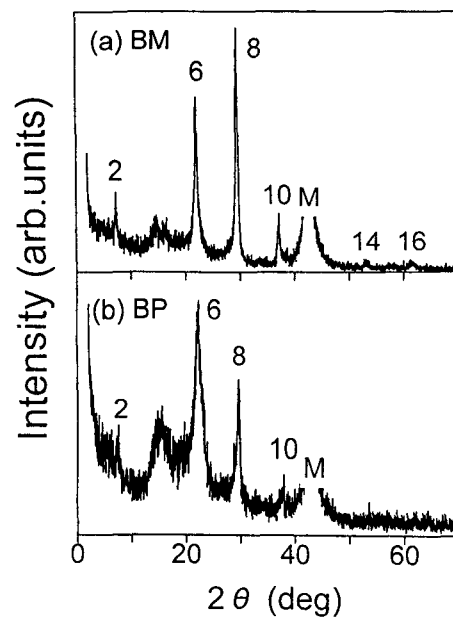


Fig.3. The XRD patterns of nondoped Bi2201, showing *c*-oriented Bi2201 phase.

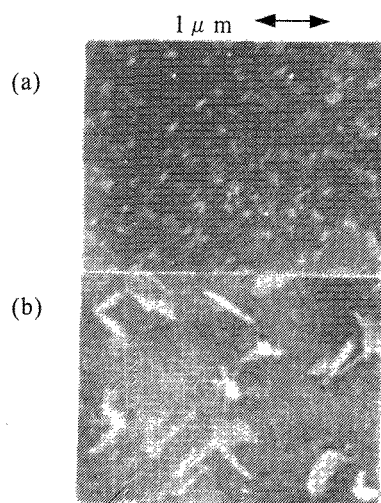


Fig.4. SEM images of nondoped Bi2201. (a) BM, (b) BP.

(006) and (008) peaks are 0.10° and 0.08° in BCP, and 0.24° and 0.32° in BCM, respectively. These results clearly indicate that the crystal growth of Ca-doped Bi2201 is enhanced and improved by the plasma. The RMS value in BCP is almost the same with that in BCM although the crystal growth is much developed in BCP. Then it can be judged that the surface is smoothed by the plasma in this case as well.

The XRD patterns of nondoped Bi2201 films are shown in Fig.3. The films of BM shown in (a) was prepared with the molecules, and BP in (b) with the plasma. The both films are c-oriented Bi2201 phases but the crystal growth is comparatively progressed in BM. The FWHM values of (006) and (008) peaks are 0.32° and 0.40° in BM, and 0.48° and 0.56° in BP, respectively. These results clearly indicate that the crystal growth of nondoped Bi2201 is enhanced and improved rather by the molecules. The SEM surface images are shown in Fig.4 for (a) BM and (b) BP. The two films show almost the same surface smoothness. To investigate their detailed surface, the AFM images were observed on them. The results are shown in Fig.5 for (a) BM and (b) BP. The crystalline nuclei are observed on the both films and the nucleation is much developed in BM. Reflecting the nucleation density, the RMS value of BM is larger than that of BP (Table I). A step of nucleus corresponds to one unit cell height (24 \AA), then the crystal growth is two dimensional nuclear growth mode. It is known from the XRD pattern in Fig.3 (b), that the flat region among the nuclei shown in Fig.5 (b) has amorphous-like structures.

We can summarize here that the growth of

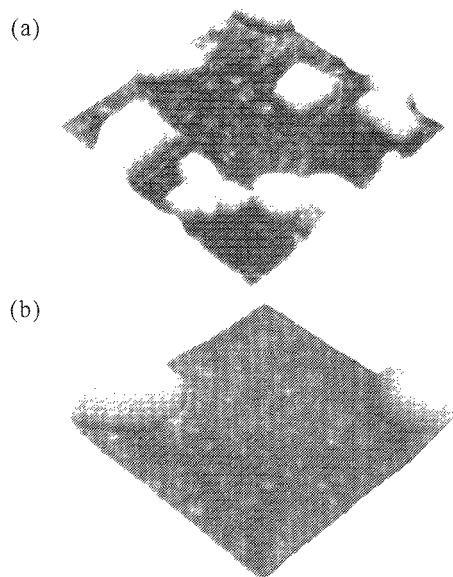


Fig.5. AFM images of nondoped Bi2201 in $1 \times 1 \mu\text{m}^2$. (a) BM, RMS=42 Å. (b) BP, RMS=22 Å.

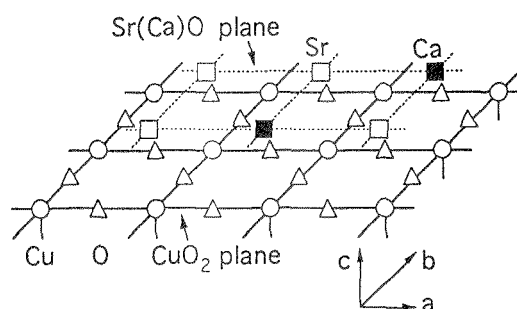


Fig.6. Atomic arrangement of Sr-Ca surface of Ca-doped Bi2201 structure.

a-YBCO and Ca-doped Bi2201 is enhanced by the plasma, whereas that of nondoped Bi2201 is enhanced by the molecules. These differences can be classified in terms of the surface energy. The a-YBCO and Ca-doped Bi2201 films have plural atom species on their growing surfaces (e.g., Y and Ba in the a-YBCO, Sr and Ca in the Ca-doped Bi2201), then their entropies are larger and their surface energies are higher. In contrast, the nondoped Bi2201 film has monoatomic layers on its growing surface (e.g., Sr-layer), then its entropy is smaller and its surface energy is lower. Therefore, it can be recognized that the plasma enhances the growth of a-YBCO and Ca-doped Bi2201 with the higher surface energies. This mechanism of the growth enhancement is interpreted for the Ca-doped Bi2201

in more detail as follows.

As shown in Fig.6, the Ca-doped Bi2201 has two kinds of atoms, say Sr and Ca, on its surface during the growth. Generally, Sr and Ca are arranged randomly then its entropy is larger and its surface energy is higher compared with the nondoped Bi2201 having a single atom species, say Sr. It is possible that Sr and Ca atoms are excited and vibrated by the oxygen plasma, and they are changed their sites with each other by jumping during the growth of Sr-Ca layer. If the higher order is introduced in the arrangement of Sr-Ca layer, the entropy and the surface energy can be reduced. This results in easier adsorptions and bondings to the growing surface for the deposited atoms. Thus the growth of Ca-doped Bi2201 can be enhanced. In fact, the growth rate of BCP is higher than that of BCM. Furthermore, according to the reduction of surface energy, the two dimensional Stranski-Krastanov growth mode dominates over the three dimensional Volmer-Weber growth mode. This leads to the smoother surface, which was already confirmed by our previous experiments. For example, the RMS value is 27 Å for the Ca-doped Bi2201 grown with the plasma having the film thickness of 600 Å. This means that the film grows with one unit cell step.⁸⁾ The introduced higher order must improve the whole crystallinity. This is also confirmed by the result that the FWHM is much smaller for BCP. The same scenario can be applied to the a-YBCO.

On the contrary, the crystal growth of nondoped Bi2201 was improved by the oxygen molecules. We suggest two possible reasons for this. One is that the nondoped Bi2201 intrinsically grows at low temperatures without strong oxidations. We have, in fact, succeeded to grow it at 400°C with the supply of oxygen molecules.⁹⁾ Watanabe et al.¹⁰⁾ reported a possibility of its growth at 300°C. The other is that the oxygen molecules are excited through collisions with the sputtered particles and their excited energy can be used to improve the crystallinity. We have demonstrated that the crystallinity of Bi2201 is further improved due to the increased collision events by introducing additional oxygen molecules between the target and substrate.⁷⁾ It can be deduced that the plasma supplies excess energy to deteriorate the crystallinity of nondoped Bi2201. However, it is expected that we can markedly improve the crystallinity of Bi2201 by optimizing the plasma condition in the future.

4. Summary

The thin films of a-YBCO, Ca-doped Bi2201 and nondoped Bi2201 were prepared by IBS and the effects of oxygen plasma supply were investigated. The crystal growth of a-YBCO and Ca-doped Bi2201 was enhanced and improved by the plasma. The surfaces of plasma-supplied films were smoother than that of molecular-supplied films. We propose that the growth

is enhanced and improved due to the reduction of surface energy during the growth by the plasma energy. The reduction of surface energy induces Stranski-Krastanov growth mode then the film surface becomes two dimensional and smoother.

The growth of nondoped Bi2201 was improved by the oxygen molecules instead. We propose that the moderate excitation energy arising from the collisions between the molecules and sputtered particles is effective for this improvement.

We thank TATEHO DEN-YU for supplying us MgO substrates.

References

- 1) "Epitaxial Oxide Thin Films III", Eds. by D. G. Schlom, C. B. Eom, M. E. Hawley, C. M. Foster, and J. S. Speck, MRS, Pittsburgh, (1997), MRS Proc. Vol. **474**.
- 2) D. G. Schlom, A. F. Marshall, J. T. Sizemore, Z. J. Chen, J. N. Eckstein, I. Bozovic, K. E. von Dessionneck, J. S. Harris Jr., and J. C. Bravman, *J. Cryst. Growth*, **102**, 361-375 (1990).
- 3) T. Endo, H. Yan, K. Abe, S. Nagase, Y. Ishida, and H. Nishiku, *J. Vac. Sci & Technol.*, **A15**, 1990-1998 (1997).
- 4) K. Sakai, S. Migita, H. Ota, H. Otera, and R. Aoki, *IEICE Trans. Electron.*, **E76-C**, 1246-1250 (1993).
- 5) M. Mukaida and S. Miyazawa, *Jpn. J. Appl. Phys.*, **32**, 4521-4528 (1993).
- 6) T. Endo, H. Yan, M. Wakuta, H. Nishiku, and M. Goto, *Jpn. J. Appl. Phys.*, **35**, L1260-L1263 (1996).
- 7) T. Endo, M. Horie, N. Hirate, K. Itoh, S. Yamada, M. Tada, K. Itoh, M. Sugiyama, S. Sano, and K. Watabe, *Jpn. J. Appl. Phys.*, **37**, L886-L889 (1998).
- 8) T. Endo (submitted).
- 9) T. Endo, H. Wakuta, M. Gotoh, N. Hirate, and M. Horie, "Advances in Superconductivity IV", Eds. by S. Nakajima and M. Murakami, Springer, Tokyo (1997) pp.1063-1066.
- 10) S. Watanabe, M. Kawai, and T. Hanada, *Jpn. J. Appl. Phys.*, **29**, L1111-L1113 (1990).

(Received December 11, 1998; accepted February 28, 1999)